

## THE REDUCTION MECHANISM OF ALLYL ALCOHOL ON IRON SURFACE AND THE EFFECT ON THE CORROSION OF IRON

A.A. AKSÜT and S. BİLCİÇ

Department of Physical Chemistry, Faculty of Science, University of Ankara/TURKEY

### ABSTRACT

In this study the corrosion of recrystallized pure iron in the sulphuric acid media and the reduction mechanism of allyl alcohol on the iron surface were investigated. For this purpose current potential curves were obtained by potentiodynamic method. The reduction of allyl alcohol on the iron surface was shown by using these curves.

### INTRODUCTION

The corrosion rates of metals and alloys can be determined by electrochemical and nonelectrochemical methods. Electrochemical methods are:

1- Extrapolating the steady state cathodic and anodic Tafel lines to  $E = E_{cor}$ .

2- The linear polarization method by the help of Stern-Geary equation.

3- Measuring the polarization resistance,  $R_p$ , using the ac technique.

In both cases 2) and 3) the measured  $R_p$  values are related to the corrosion current density according to the Stern-Geary equation:

$$i_{cor} = \frac{b_a \cdot b_c}{2.303 (b_a + b_c)} \cdot \frac{1}{R_p} = \frac{B}{R_p} \quad (1)$$

Where  $b_a$  and  $b_c$  represent the anodic and cathodic Tafel slopes respectively. Non electrochemical methods include.

1- measuring the decrease of weight and

2- solution analysis.

In this study corrosion rates were obtained by extrapolating the cathodic and anodic Tafel lines to  $E = E_{\text{cor}}$ . The reduction of PA to ALA was shown in literature (Aksüt, A.A. et al, 1982; Aksüt, A.A., 1982 and Aksüt, A.A., 1983). In some studies PA is proposed to be reduced to the single bond (Poling, G.W., 1967; Tedeschi, R.J., 1975; Hausler R.H., 1977). Hence, in this study, it was investigated whether the reduction of allyl alcohol takes place on the iron surface or not and it was shown that allyl alcohol could be reduced up to the single bond.

## EXPERIMENTAL

The investigations were carried out in the following systems  $\text{Fe}^* / x\text{M H}_2\text{SO}_4 + y\text{M Na}_2\text{SO}_4 + z\text{mM ALA}^{**}$

using by purified nitrogen (passed through liquid nitrogen), rotating disc technique at a rotation frequency of 30 rps. Saturated calomel and Pt foil electrodes were used as reference and counter electrodes. The electrode was polished with sandpaper and washed with bidistilled water. The solution were also prepared by bidistilled water.

## EXPERIMENTAL RESULTS

The current density-potential curves measured by linear potential sweep technique in deaerated  $0.5\text{M H}_2\text{SO}_4 + z\text{mM ALA}$  ( $\text{pH} = 0.7$ ),  $0.05\text{M H}_2\text{SO}_4 + 0.45\text{M Na}_2\text{SO}_4 + z\text{mM ALA}$  ( $\text{pH} = 1.7$ ) and  $0.005\text{M H}_2\text{SO}_4 + 0.495\text{M Na}_2\text{SO}_4 + z\text{mM ALA}$  ( $\text{pH} = 2.7$ ) solutions are given in Figs 1, 2 and 3 respectively. The potential sweep was started at  $E = E_{\text{cor}}$  and then the curves were obtained first in cathodic and then anodic directions using a sweep rate of  $1 \text{ mVs}^{-1}$ . For each system at different pH values, cathodic Tafel slopes were obtained to be  $b_c = -120 \pm 10 \text{ mV}$  in the ALA-free systems while  $b_c = -200 \pm 20 \text{ mV}$  in the ALA containing systems. Anodic Tafel slopes were determined to be  $b_a = 45 \pm 5 \text{ mV}$  for each system.

Figure 4 shows the variation of  $\log i$  with respects to  $\log C_{\text{ALA}}$  at constant potential and constant pH. In this figure the three lines are parallel to each other and the slope is approximately 0.26 - 0.28. At constant potential and constant  $C_{\text{ALA}}$  the variation of  $\log i$  with pH

\* The electrode kept at  $1050^\circ\text{C}$  for two hours recrystallized by cooling with a rate of  $150^\circ\text{C}/\text{hour}$ , having a purity of 99.999 %.

\*\* Freshly distilled allyl alcohol.

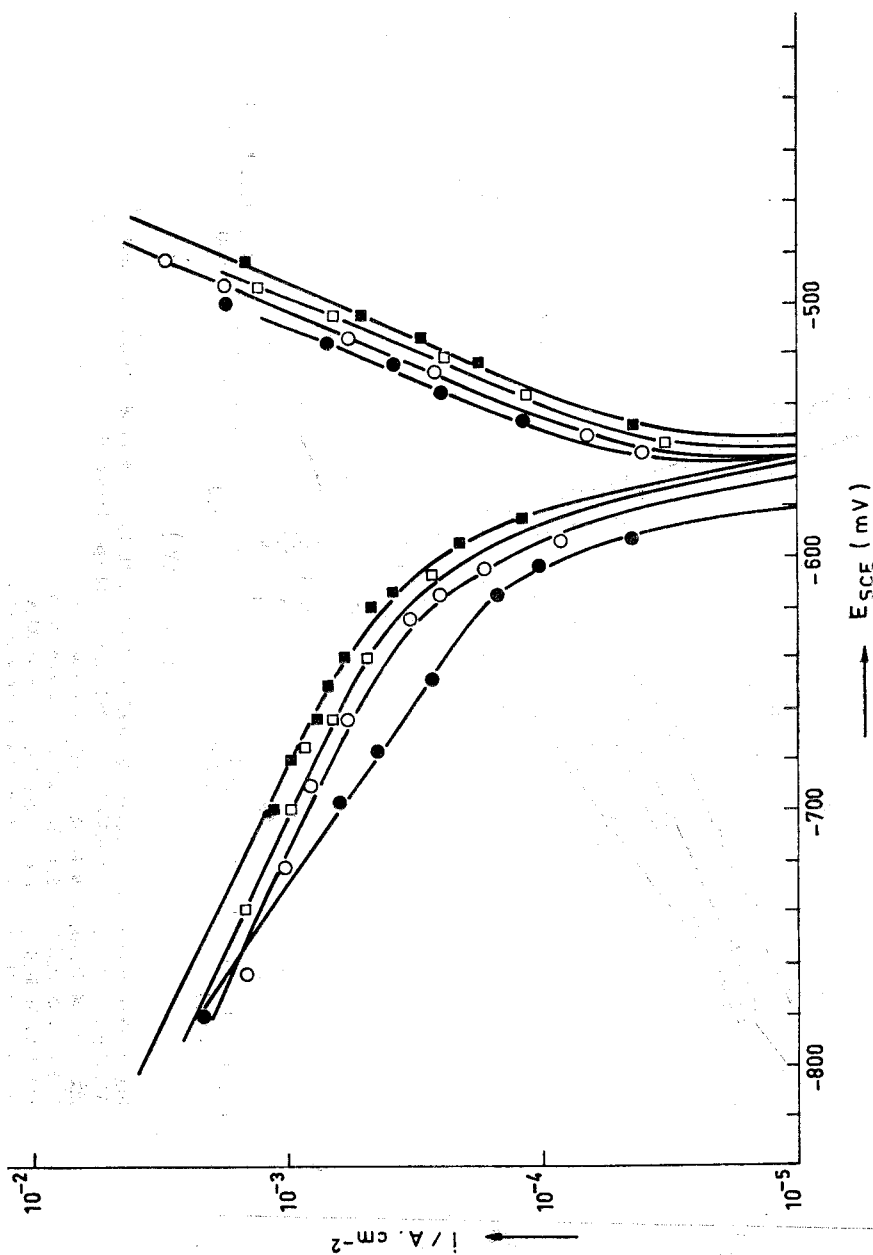


Fig. 1. Current-potential curves obtained in 0.5 M  $\text{H}_2\text{SO}_4$  + zmM ALA (pH = 0.7).  
 $v = 1 \text{ mVs}^{-1}$ ,  $T = 298^\circ\text{K}$ ,  $v = 30 \text{ rps}$ , deaerated  
 (●) 0.5 M  $\text{H}_2\text{SO}_4$  + 0mM ALA; (○) 0.5 M  $\text{H}_2\text{SO}_4$  + 1mM ALA;  
 (□) 0.5 M  $\text{H}_2\text{SO}_4$  + 2mM ALA; (■) 0.5 M  $\text{H}_2\text{SO}_4$  + 10mM ALA.

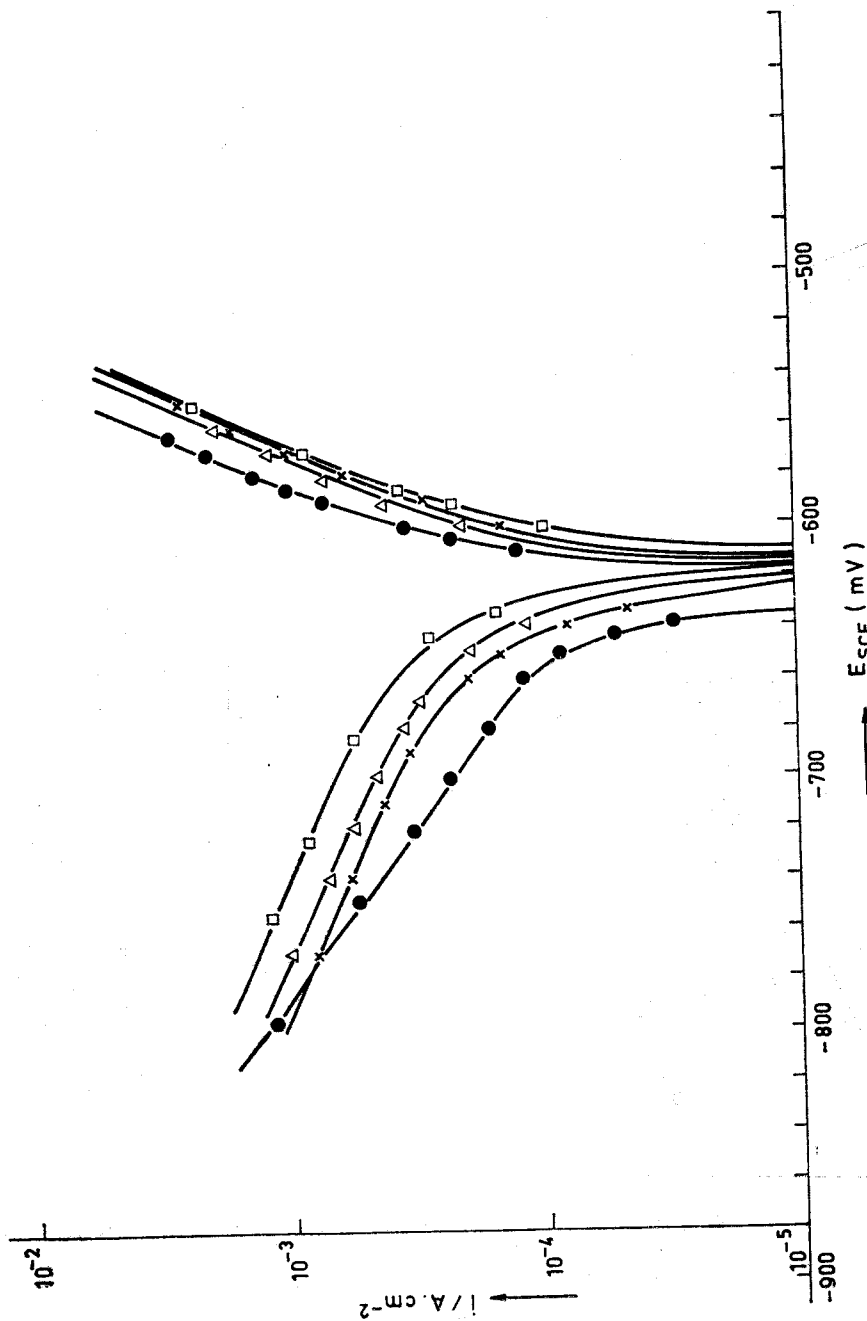


Fig. 2. Current-potential curves obtained in 0.05 M  $\text{H}_2\text{SO}_4$  + 0.45 M  $\text{Na}_2\text{SO}_4$  + zinc ALA (pH = 1.7),  $v = 1 \text{ mVs}^{-1}$ ,  $T = 298^\circ\text{K}$ ,  $v = 30 \text{ rps}$ , deaerated  
 (●) 0.05 M  $\text{H}_2\text{SO}_4$  + 0.45 M  $\text{Na}_2\text{SO}_4$  + 0.05 mM ALA;  
 (×) 0.05 M  $\text{H}_2\text{SO}_4$  + 0.45 M  $\text{Na}_2\text{SO}_4$  + 1 mM ALA;  
 (Δ) 0.05 M  $\text{H}_2\text{SO}_4$  + 0.45 M  $\text{Na}_2\text{SO}_4$  + 2 mM ALA;  
 (○) 0.05 M  $\text{H}_2\text{SO}_4$  + 0.45 M  $\text{Na}_2\text{SO}_4$  + 10 mM ALA

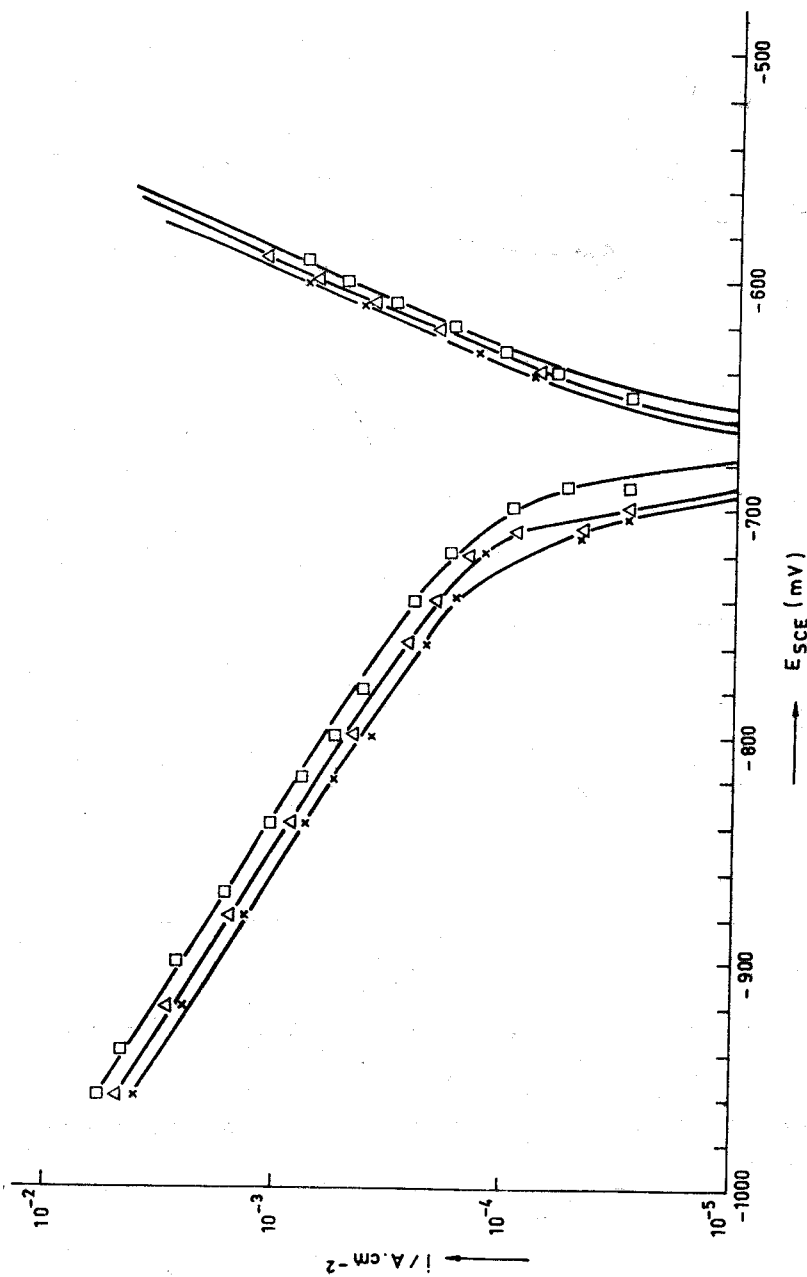


Fig. 3. Current-potential curves obtained in 0.005 M  $\text{H}_2\text{SO}_4$  + 0.495 M  $\text{Na}_2\text{SO}_4$  + 2 mM ALA (pH = 2.7),  $v = 1 \text{ mV s}^{-1}$ ,  $T = 298^\circ\text{K}$ ,  $v = 30 \text{ rps}$ , deaerated  
 (×) 0.005 M  $\text{H}_2\text{SO}_4$  + 0.495 M  $\text{Na}_2\text{SO}_4$  + 1 mM ALA;  
 (Δ) 0.005 M  $\text{H}_2\text{SO}_4$  + 0.495 M  $\text{Na}_2\text{SO}_4$  + 2 mM ALA;  
 (□) 0.005 M  $\text{H}_2\text{SO}_4$  + 0.495 M  $\text{Na}_2\text{SO}_4$  + 10 mM ALA.

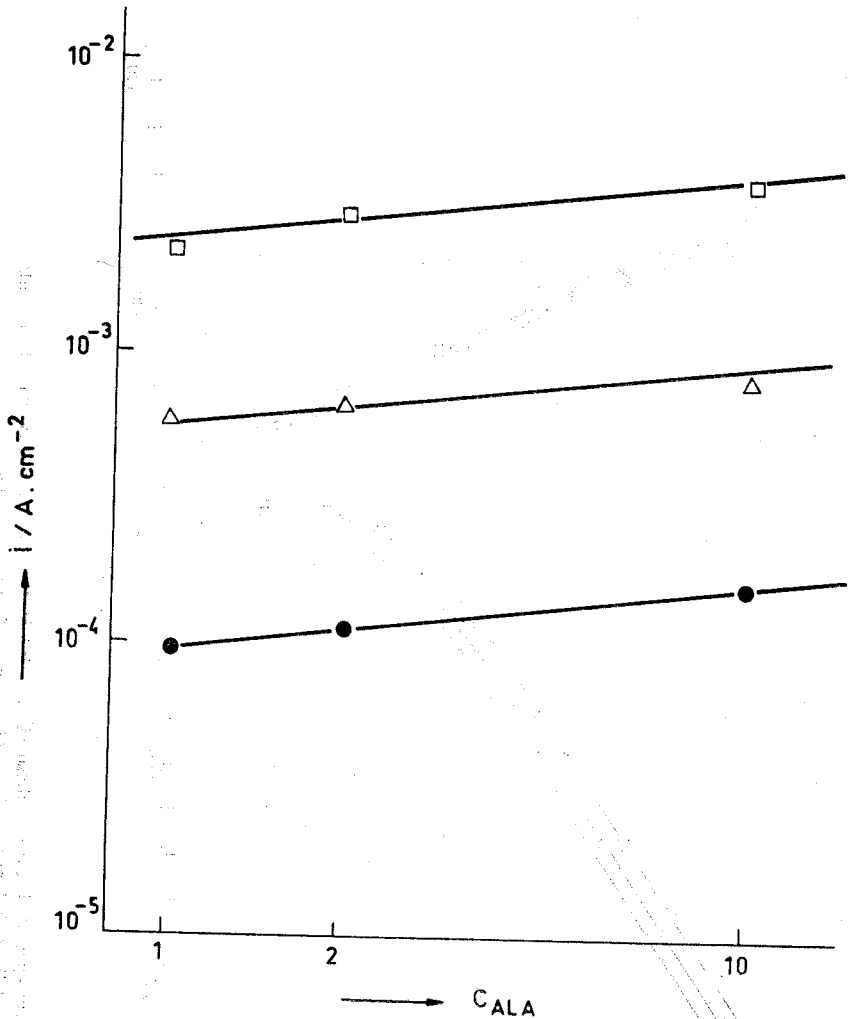


Fig. 4. The variation of  $\log C_{ALA}$  with  $\log i$  at constant potential. ( $\square$ ) pH = 0.7; ( $\Delta$ ) pH = 1.7; ( $\bullet$ ) pH = 2.7. T = 298°K,  $\nu$  = 30 rps, deaerated

can be seen in Figure 5. The lines obtained are also parallel to each other and the slope is around 0.56 - 0.60.

## DISCUSSION AND RESULTS

The reaction order can be calculated from the plot of  $\log i$  vs  $\log C_{ALA}$  at constant potential and constant pH (Fig. 4). The calculated reaction order according to ALA concentration is

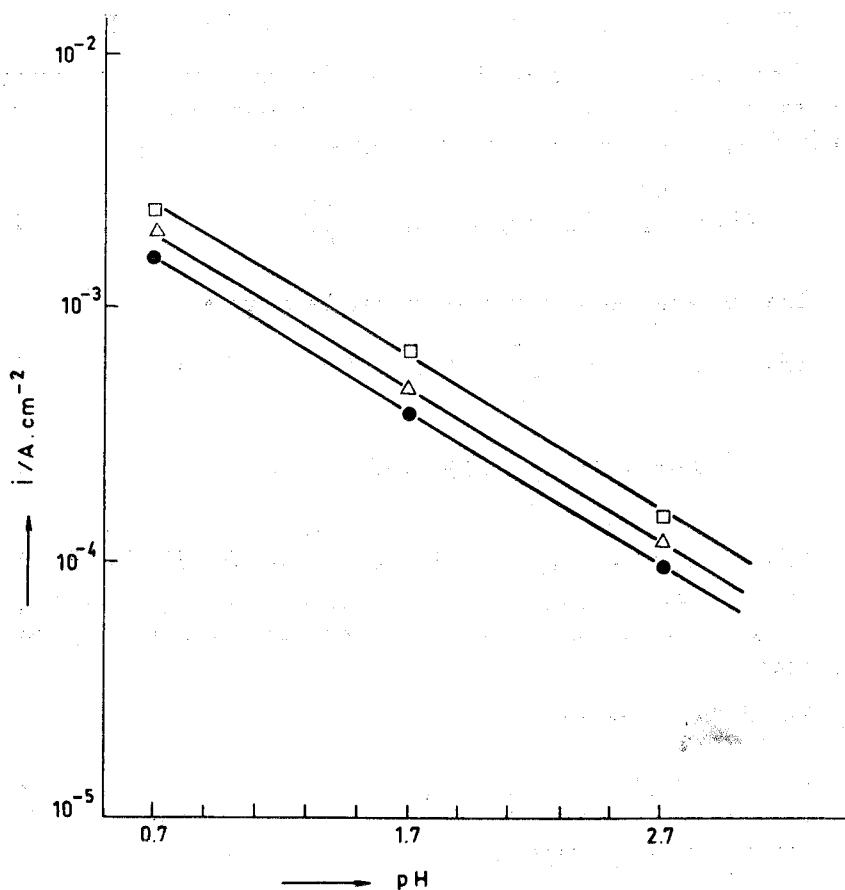


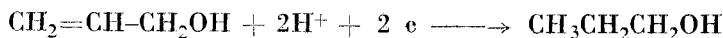
Fig. 5. The variation of  $\log i$  with pH at constant  $C_{ALA}$ . (●) 1 mM ALA; (Δ) 2 mM ALA; (□) 10 mM ALA.  $T = 298^\circ K$ ,  $\nu = 30$  rps, deaerated.

$$\left( \frac{\partial \log i}{\partial \log C_{ALA}} \right)_{E, pH} = 0.28$$

The reaction order according to the  $H^+$  can be determined from the plot of  $\log i$  vs pH at constant  $C_{ALA}$  and constant potential in the cathodic zone. From Fig. 5 this value was found to be.

$$\left( \frac{\partial \log i}{\partial pH} \right)_{E, C_{ALA}} = -0.56$$

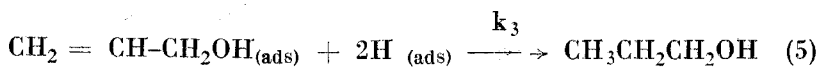
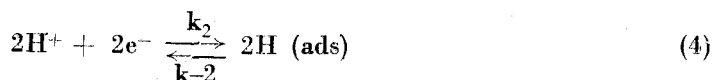
According to these results it can be seen that ALA should be reduced to  $CH_3CH_2CH_2OH$  according to the following equation.



From these kinetic parameters, the following equation describing the reduction rate of ALA to propanol on iron electrodes in acidic media is obtained within the potential range studied.

$$i_- = -2F \cdot k_- \cdot C_{\text{ALA}} \cdot C_{\text{H}^+}^{0,28} \exp\left(-\alpha_{\text{cath}} \frac{FE}{RT}\right) \quad (2)$$

The following reaction mechanism can be proposed



The following equations can be written for reactions (3) and (4) at the Temkin adsorption conditions (CELDRAN, R and et al, 1981 and 1981).

For the 3 rd reaction:

$$e - \frac{r_{\text{ALA}} \cdot \theta_{\text{ALA}}}{RT} = K_1 C_{\text{ALA}} \quad (6)$$

and for the 4 th reaction,

$$e - \frac{r_{\text{H}} \cdot \theta_{\text{H}}}{RT} = K_2 C_{\text{H}^+}^2 \exp\left(-\frac{FE}{RT}\right) \quad (7)$$

From the rate determining step (5) the following equation can be written

$$v_3 = -k_3 \theta_{\text{ALA}} \theta_{\text{H}}^2 \exp\left[-\frac{\gamma (r_{\text{ALA}} \cdot \theta_{\text{ALA}} + r_{\text{H}} \cdot \theta_{\text{H}})}{RT}\right] \quad (8)$$

Multiplying the right and left sides of (6) and (7) and raising to power  $\gamma$ : the following equation is obtained.

$$\exp\left[-\frac{\gamma (r_{\text{ALA}} \cdot \theta_{\text{ALA}} + r_{\text{H}} \cdot \theta_{\text{H}})}{RT}\right] = (K_1 K_2)^\gamma C_{\text{ALA}}^\gamma C_{\text{H}^+}^{2\gamma} \exp\left(-\frac{\gamma FE}{RT}\right) \quad (9)$$



From (8) and (9) the following equation is obtained for the reaction rate

$$i_c = -2 FK \frac{C_{ALA}^\gamma}{C_{H^+}^{2\gamma}} \exp\left(-\frac{\gamma FE}{RT}\right) \quad (10)$$

where

$$K = k_3 (K_1 K_2) \theta_{ALA} \theta_{H^+}^2$$

Equation (10) completely agrees with (2) if  $\gamma = 0.28$ . Under this condition, the cathodic Tafel slope is

$$\left(\frac{\partial E}{\partial \log i}\right)_{pH} = -\frac{2,303 RT}{\gamma F} = -207 \text{ mV.}$$

This value is in complete compliance with the experimental value obtained ( $b_c = -200 \pm 20 \text{ mV}$ ).

The variation of  $i_{cor}$  with  $\log C_{ALA}$  at constant pH and with pH at constant  $C_{ALA}$  are given in Figs. 6 and 7 respectively.

These experimental data show that ALA is reduced to propanol according to the given reaction mechanism.

## ÖZET

Bu çalışmada yeniden kristallendirilmiş saf demirin (% 99,999) alil alkol içeren sülfürik asit ortamındaki korozyonu, alil alkolün (ALA) redüksiyonu ve redüksiyon mekanizması incelenmiştir. Bu amaçla potansiyodinamik yöntemle ( $dE/dt = 1 \text{ mV/s}$ ) akım-potansiyel eğrileri elde edilmiştir. Bu eğrilerden ALA'nın demir yüzeyinde redüklendiği gösterilmiştir.

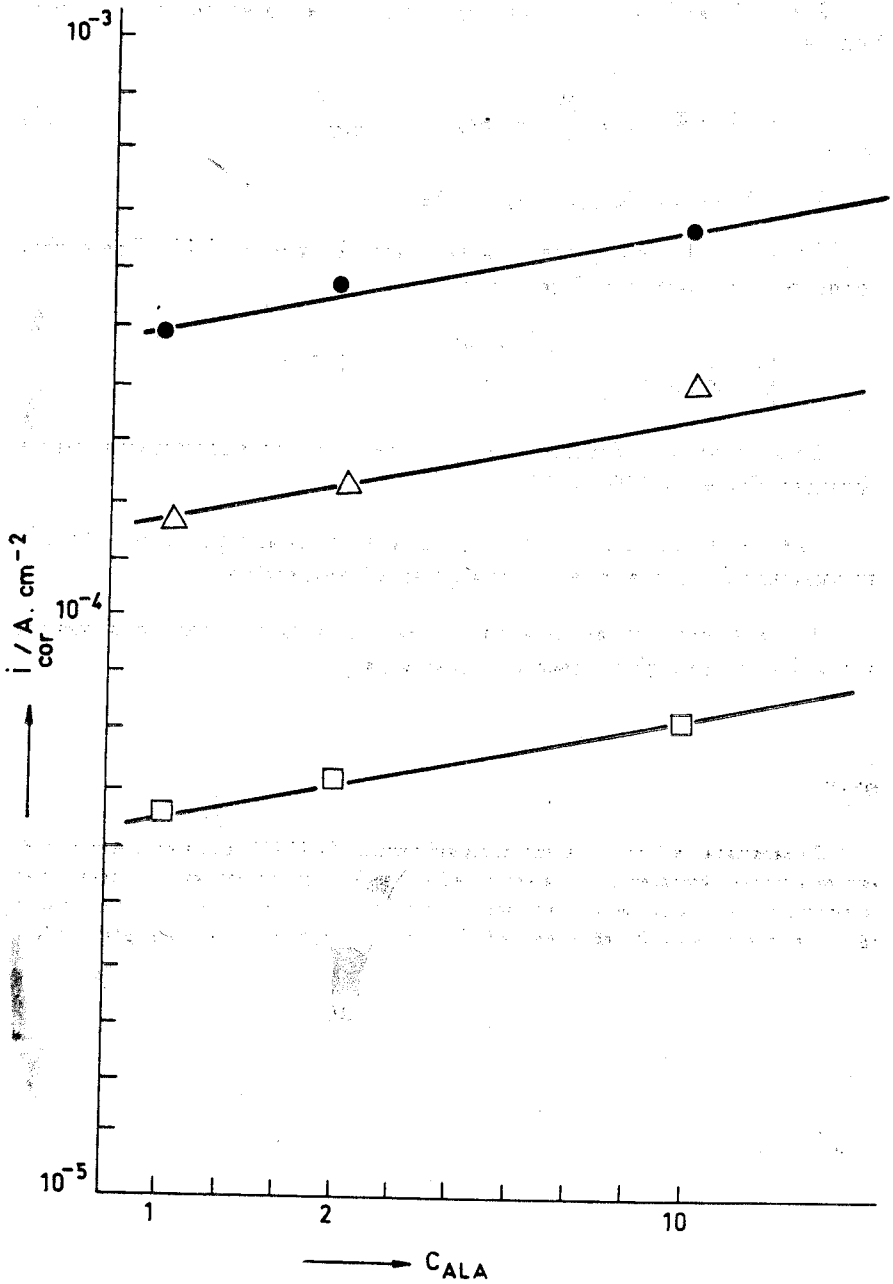


Fig. 6. The variation of  $\log i_{cor}$  with  $\log C_{ALA}$  at constant pH. (□) 1mM ALA; (Δ) 2mM ALA; (●) 10 mM ALA.  $T = 298^{\circ}K$ ,  $\nu = 30$  rps, deaerated.

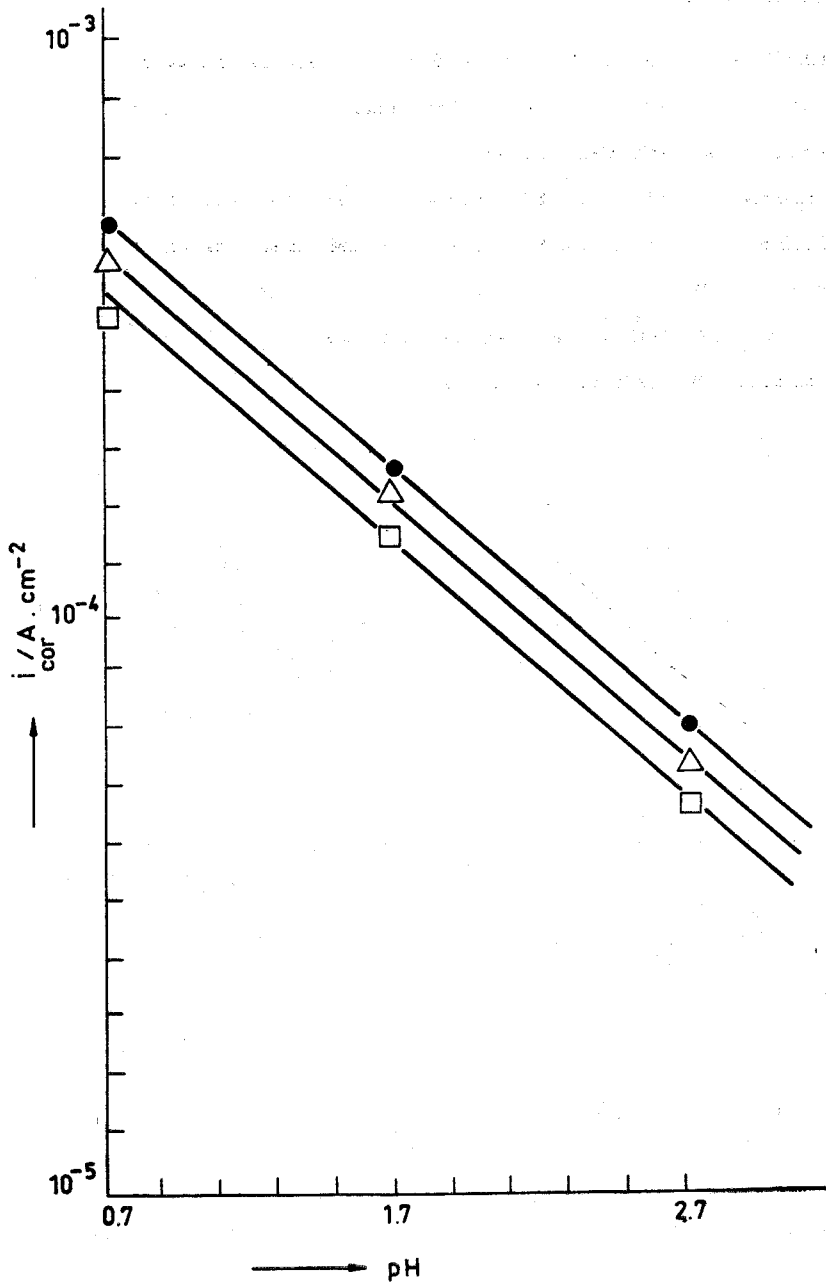


Fig. 7. The variation of  $\log i_{cor}$  with pH at constant  $C_{ALA}$ . ( $\square$ ) 1 mM ALA; ( $\Delta$ ) 2 mM ALA; ( $\bullet$ ) 10 mM ALA.  $T = 298^\circ K$ ,  $\nu = 30$  rps, deaerated.

## REFERENCES

- AKSÜT, A.A., LORENZ, W.J. and MANSFELD, F., 1982. *Cor. Sci.* 22, 611.
- AKSÜT, A.A., 1982. *Comm. Fac. Sci. Univ. Ankara.*
- AKSÜT, A.A., 1983. *Elec. Acta*, 28, 1177.
- CELDRAÑ, R. and GONZALEZ - VELASCO, J., 1981. *Elec. Acta*, 26, 525.
- CELDRAÑ, R. and GONZALEZ - VELASCO, J., 1981. *Elec. Acta*, 26, 763.
- HAUSLER, R.H., 1977. *Corrosion*, 33, 117.
- POLING, G.W., 1967. *J. Electrochem. Soc.*, 114, 1209.
- TEDESCHI, R.J. 1975. *Corrosion*, 3, 130.